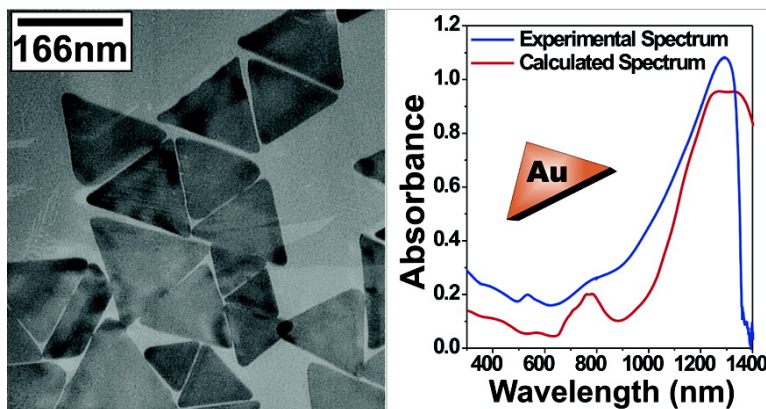


## Observation of a Quadrupole Plasmon Mode for a Colloidal Solution of Gold Nanoprisms

Jill E. Millstone, Sungho Park, Kevin L. Shuford, Lidong Qin, George C. Schatz, and Chad A. Mirkin

*J. Am. Chem. Soc.*, **2005**, 127 (15), 5312-5313 • DOI: 10.1021/ja043245a • Publication Date (Web): 26 March 2005

Downloaded from <http://pubs.acs.org> on March 25, 2009



### More About This Article

Additional resources and features associated with this article are available within the HTML version:

- Supporting Information
- Links to the 51 articles that cite this article, as of the time of this article download
- Access to high resolution figures
- Links to articles and content related to this article
- Copyright permission to reproduce figures and/or text from this article

[View the Full Text HTML](#)

## Observation of a Quadrupole Plasmon Mode for a Colloidal Solution of Gold Nanoprisms

Jill E. Millstone, Sungho Park, Kevin L. Shuford, Lidong Qin, George C. Schatz, and Chad A. Mirkin\*

*Department of Chemistry and Institute for Nanotechnology, Northwestern University, 2145 Sheridan Road, Evanston, Illinois 60208-3113*

Received November 9, 2004; E-mail: camirkin@chem.northwestern.edu

The use of nanostructured materials in applications such as biodetection,<sup>1</sup> catalysis,<sup>2</sup> and electronics<sup>3</sup> has led to an explosion of interest in the development of synthetic methods for preparing such structures. The majority of effort thus far has focused on isotropic, pseudo-spherical structures, but recently, researchers have made promising advances that are yielding control over particle size, shape, and composition.<sup>1–4</sup> These architectural parameters dictate the physical and chemical properties of a nanostructure.<sup>5</sup>

Triangular nanoprisms, in particular, are a class of nanostructures that have generated intense interest due to their unusual optical properties and the recent development of new methods for preparing bulk quantities of them.<sup>4</sup> Depending upon composition and desired dimensions, certain types of prisms can be prepared either thermally or photochemically.<sup>4a,b</sup> The photochemical routes, thus far, have been used to synthesize silver nanoprisms with excellent size control. Gold nanoprisms, on the other hand, have been synthesized exclusively by thermal methods with varying degrees of success regarding purity and size control.<sup>6,7</sup> Both prism compositions are particularly attractive for their enhancing properties with respect to Raman spectroscopy. The optical spectra of nanoprisms should exhibit a distinct dipole resonance as observed in isotropic spherical structures in addition to weaker higher order resonances.<sup>8</sup> In the case of silver, where bulk preparations of high quality and relatively pure nanoprisms can be realized, these plasmons have been identified and assigned through experiment and computation.<sup>4a</sup> To the best of our knowledge, no one has experimentally identified a quadrupole resonance for colloidal solutions of gold nanoprisms. Such structures should exhibit quadrupole resonances as evidenced by their identification in lithographically patterned analogues.<sup>9</sup> The identification of higher order surface plasmon resonance modes with other metal nanoparticles is important because it provides not only greater understanding of their physical properties but also a spectroscopic fingerprint that can be used to characterize and assess the quality of such structures. Herein, we present a synthetic approach and separation procedure for synthesizing and isolating large quantities of gold nanoprisms with uniform edge lengths and thicknesses, which has allowed us to use UV–vis–NIR spectroscopy to observe an in-plane quadrupole resonance mode of such structures for the first time.

Our synthetic procedure builds off the work of Murphy et al.<sup>10</sup> and involves the preparation of small gold seed nanoparticles ( $d = 5.2 \pm 0.6$  nm) and the subsequent three-step growth of seeds in an aqueous solution containing the capping agent (cetyltrimethylammonium bromide (CTAB)), gold ions ( $\text{HAuCl}_4 \cdot 3\text{H}_2\text{O}$ ), reducing agent (ascorbic acid), and NaOH (see Supporting Information). This synthetic procedure produces a mixture of spherical and triangular gold nanoparticles, each with a relatively homogeneous size distribution (Figure 1A). In contrast with many other similar synthetic routes for gold nanostructures utilizing CTAB, our synthetic method produced no rods, cubes, or branched structures.<sup>10c</sup>

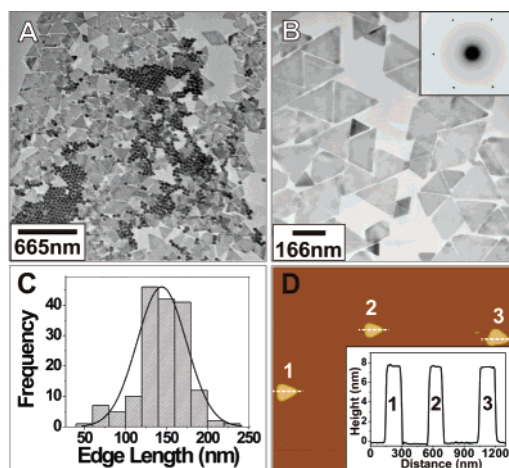


**Figure 1.** (A) TEM image of Au spherical and triangular nanoparticles. (B) Zoom-in image. Inset shows the electron diffraction pattern of the top of a single prism. (C) Histogram of nanoprisms edge lengths. (D) AFM image of nanoprisms on mica (tapping mode). Inset: height profile along the dashed lines.

The histogram in Figure 1C represents the edge-length size distribution of the nanoprisms. The average edge length of the nanoprisms is  $144 \pm 30$  nm. We also measured the average spherical nanoparticle diameter and found that it is  $35 \pm 2$  nm. Interestingly, electron diffraction analysis of an individual gold nanoprism shows that, unlike lithographically generated structures, they are single crystalline and that the large, flat top and bottom faces are [111] facets (Figure 1B). Atomic force microscope (AFM) images of the gold nanoprisms confirm that their top and bottom faces are atomically flat with a uniform thickness of  $7.8 \pm 0.5$  nm (13 prisms studied, Figure 1D and inset). This thickness is approximately equal to the average diameter of the seed nanoparticles when the thickness of the two layers of CTAB on the top and bottom surfaces of nanoprisms is taken into account. This suggests that growth of prisms occurs in two dimensions from the isotropic seed to form the anisotropic prism.

The nanoprism growth process has been monitored in real time by UV–vis–NIR spectroscopy (Figure 2). The spectra clearly reveal two distinct bands, the first of which appears at 532 nm and indicates the presence of spherical particles ( $35 \pm 2$  nm, Figure 1A). The position of this band does not change significantly with time. The band is assigned to the dipole resonance associated with the spherical gold nanoparticles and its intensity correlates with the concentration of gold nanoparticles in solution. A second band is observed initially at 750 nm, and this band red-shifts as the growth process continues. This band is assigned to the dipole resonance of the gold nanoprisms, and at the end of the growth process it appears in the NIR at 1296 nm in conjunction with another band that appears at 814 nm. The shift of  $\lambda_{\text{max}}$  most likely reflects an

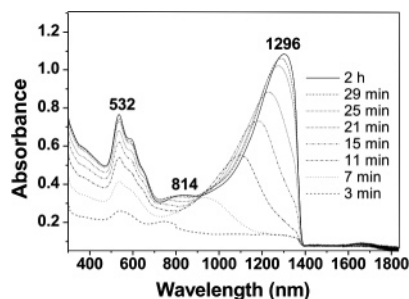


**Figure 2.** In situ UV-vis-NIR spectra following the formation of gold nanoparticles after seed addition.

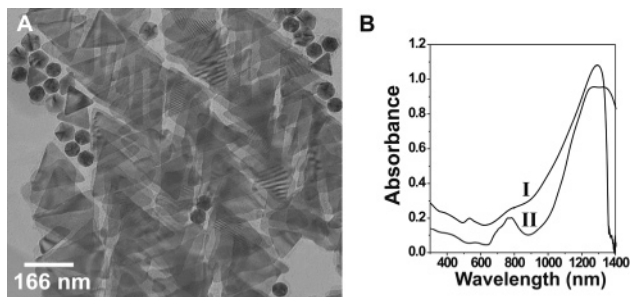


**Figure 3.** (A) TEM image of the purified Au nanoprisms. (B) Corresponding UV-vis-NIR spectra of purified Au nanoprisms (I) and DDA calculation (II).

increase in nanoprism edge length.<sup>8</sup> The assignment of this shift in dipole resonance as a function of time and concomitant increase in edge length is consistent with theoretical calculations and our isolation of the final nanoprism product (vide infra). After 30 min the reaction stops as indicated by fixed dipole plasmon resonances at 532 nm for the spherical particle products and at  $\sim 1300$  nm for the nanoprisms. These bands do not increase in intensity after this point, even after three months in the growth solution. The nanoprisms can be separated from the spherical nanoparticles by using an aluminum oxide filter with 100-nm pore sizes. Interestingly, when the nanoprisms are predominantly separated from the spherical particles, one clearly sees a broad band in their UV-vis-NIR spectrum at 800 nm, which we assign to the in-plane quadrupole mode of the nanoprisms (Figure 3). This assignment is based upon the characterization of these prisms by electron microscopy and on discrete dipole approximation (DDA) calculations,<sup>11</sup> which predict plasmon bands that match experiment.

Significantly, a UV-vis-NIR spectrum (I) of the purified Au nanoprisms and a corresponding simulated spectrum obtained by DDA calculations (II) are in excellent agreement (Figure 3B). An in-plane dipole band with  $\lambda_{\text{max}} \approx 1300$  nm is observed in both spectra, as is a quadrupole band occurring at  $\lambda_{\text{max}} \approx 800$  nm. The theoretical spectrum presented in trace II reflects the experimentally derived size distribution of gold nanoprisms in solution. DDA calculations have been performed on nanoprisms with a thickness of 7.5 nm and effective edge lengths of 90, 110, 130, 150, 170, 190, and 210 nm. The contribution of each of the prisms in the set was then weighted according to a Gaussian fit of the relative particle populations in solution like that shown in Figure 1C. The weighted cross sections of these spectra were summed to form trace II. In the assignment of the quadrupole resonance, the possible contribu-

tions from nanoprisms of smaller edge lengths have been considered. DDA calculations modeling relative populations of each prism length show that the intensity of the quadrupole resonance from large prisms is much greater than the intensity of the dipole resonance of any remaining small edge length prisms in solution (see Supporting Information). The asymmetry of the experimental dipole resonance peak at  $\sim 1300$  nm is due to the truncation of the peak by the absorbance of water in the IR region. It should be noted that additional calculations also showed that the in-plane dipole resonance peak at  $\sim 1300$  nm is very sensitive to the physical dimensions of Au nanoprisms, as it is in the case of Ag nanoprisms.<sup>4d,8</sup> The in-plane quadrupole is also affected by those variations, but less sensitively. For example, the resonance bands (either of Ag or Au) red-shift with increase in edge length and sharpness and decrease in thickness.<sup>8</sup>

This communication provides a method for synthesizing Au nanoprisms in their purest form. The purity of such materials has allowed us to correlate their structure with their optical properties and identify the quadrupole plasmon resonance, which has never been observed in solution because of inhomogeneity and impurities found in the products formed from other preparatory procedures. In view of the high stability of gold as compared with silver, these structures should provide a route to synthesizing many technologically useful materials not attainable with their less noble analogue.

**Acknowledgment.** C.A.M. acknowledges the NSF and ONR for support of this research. G.C.S. acknowledges the DOE (DEFG02-02-ER15487) for support of this research.

**Supporting Information Available:** Details on the nanoprism synthesis and calculation data. This material is available free of charge via the Internet at <http://pubs.acs.org>.

## References

- (1) (a) Bauer, L. A.; Birenbaum, N. S.; Meyer, G. J. *J. Mater. Chem.* **2004**, *14*, 517–526. (b) Bruchez, M.; Moronne, M.; Gin, P.; Weiss, S.; Alivisatos, A. P. *Science* **1998**, *281*, 2013–2016. (c) Nam, J. M.; Thaxton, C. S.; Mirkin, C. A. *Science* **2003**, *301*, 1884–1886. (d) Han, M. Y.; Gao, X. H.; Su, J. Z.; Nie, S. *Nat. Biotechnol.* **2001**, *19*, 631–635. (e) Elghanian, R.; Storhoff, J. J.; Mucic, R. C.; Letsinger, R. L.; Mirkin, C. A. *Science* **1997**, *277*, 1078–1081.
- (2) (a) Jana, N. R.; Pal, T. *Langmuir* **1999**, *15*, 3458–3463. (b) Jana, N. R.; Sau, T. K.; Pal, T. *J. Phys. Chem. B* **1999**, *103*, 115–121. (c) Ghosh, S. K.; Kundu, S.; Mandal, M.; Pal, T. *Langmuir* **2002**, *18*, 8756–8760.
- (3) (a) Sun, S. H.; Murray, C. B.; Weller, D.; Folks, L.; Moser, A. *Science* **2000**, *287*, 1989–1992. (b) Wang, J. F.; Gudiksen, M. S.; Duan, X. F.; Cui, Y.; Lieber, C. M. *Science* **2001**, *293*, 1455–1457.
- (4) (a) Jin, R.; Cao, Y.; Mirkin, C. A.; Kelly, K. L.; Schatz, G. C.; Zheng, J. G. *Science* **2001**, *294*, 1901–1903. (b) Sun, Y.; Mayers, B.; Xia, Y. *Nano Lett.* **2003**, *3*, 675–679. (c) Jin, R. C.; Cao, Y. C.; Hao, E. C.; Mettraux, G. S.; Schatz, G. C.; Mirkin, C. A. *Nature* **2003**, *425*, 487–490. (d) Letsinger, D. L.; Mucic, R. R.; Storhoff, J. J.; Mirkin, C. A. *Nature* **1996**, *382*, 607–609.
- (5) Link, S.; El-Sayed, M. A. *J. Phys. Chem. B* **1999**, *103*, 8410–8426.
- (6) Kim, F.; Connor, S.; Song, H.; Kuykendall, T.; Yang, P. *Angew. Chem., Int. Ed. Engl.* **2004**, *43*, 3673–3677.
- (7) Shankar, S. S.; Rai, A.; Ankamwar, B.; Singh, A.; Ahmad, A.; Sastry, M. *Nat. Mater.* **2004**, *3*, 482–488.
- (8) Kelly, K. L.; Coronado, E.; Zhao, L. L.; Schatz, G. C. *J. Phys. Chem. B* **2003**, *107*, 668–677.
- (9) Haynes, C.; McFarland, A. D.; Zhao, L. L.; Van Duyne, R. P.; Schatz, G. C.; Gunnarsson, L.; Prikulis, J.; Kasemo, B.; Kall, M. *J. Phys. Chem. B* **2003**, *107*, 7337–7342.
- (10) (a) Busbee, B.; Obare, S.; Murphy, C. J. *Adv. Mater.* **2003**, *15*, 414–416. (b) Jana, N.; Gearheart, L.; Murphy, C. J. *J. Chem. Mater.* **2001**, *13*, 2313–2322. (c) Sau, T. K.; Murphy, C. J. *J. Am. Chem. Soc.* **2004**, *126*, 8648–8649.
- (11) Draine, B. T.; Flatau, P. J. *J. Opt. Soc. Am. A* **1994**, *11*, 1491–1499.

JA043245A